

1 Article

2 Real Time Elbow Angle Estimation Using Single 3 RGB Camera

4 Muhammad Yahya¹, Jawad Ali Shah^{1,*}, Arif Warsi², Kushsairy Kadir¹, Sheroz Khan³, M Izani⁴

5 1 British Malaysian Institute, Universiti Kuala Lumpur

6 2 Malaysian Institute of Information Technology, Universiti Kuala Lumpur

7 3 Dept. of ECE, Faculty of Eng., International Islamic University, Malaysia

8 4 Visual & Digital Production Department, College of Architecture, Effat University, Jeddah, KSA

9 * Correspondence: jawad@unikl.edu.my; Tel.: +60-1121215451

10

11 **Abstract:** The use of motion capture has increased from last decade in a varied spectrum of
12 applications like film special effects, controlling games and robots, rehabilitation system, animations
13 etc. The current human motion capture techniques use markers, structured environment, and high
14 resolution cameras in a dedicated environment. Because of rapid movement, elbow angle estimation
15 is observed as the most difficult problem in human motion capture system. In this paper, we take
16 elbow angle estimation as our research subject and propose a novel, markerless and cost-effective
17 solution that uses RGB camera for estimating elbow angle in real time using part affinity field. We
18 have recruited five (5) participants of (height, 168 ± 8 cm; mass, 61 ± 17 kg) to perform cup to mouth
19 movement and at the same time measured the angle by both RGB camera and Microsoft Kinect. The
20 experimental results illustrate that markerless and cost-effective RGB camera has a median RMS
21 errors of 3.06° and 0.95° in sagittal and coronal plane respectively as compared to Microsoft Kinect.

22 **Keywords:** Angle Estimation; Microsoft Kinect; Single Camera; markerless Mocap system

23

24 1. Introduction

25 Human anatomical parts movement are captured and analyzed for various purposes such as
26 controlling games and robots [1], interaction with human machine interface [2], and neurological
27 rehabilitation [3] etc. To track and record the human body parts movement, markers and markerless
28 techniques are used which are then processed using computer. The marker based systems such as
29 Inertial Measurement Units (IMU), Vicon, Qualisys and BTS Smart-D use edges, colors, skin, and
30 wearable gloves etc. as markers while markerless systems are usually based on Ms Kinect [4]. The
31 markers used in most common optical motion capture techniques [5, 6] require controlled
32 environment and placing markers, which are time consuming. These marker based systems have the
33 limitations of mobility, being expensive and difficult to setup [6]. Recently, motion of human body
34 parts have been investigated and analyzed with several different motion capture devices in stroke
35 rehabilitation procedures [7, 8, 11, 12].

36 There have been numerous attempts to model the human upper limb body segments and
37 measure its orientation with IMU. In [7], researchers have proposed alignment free and self-
38 calibrated method for measuring the elbow angle with initial zero reference pose using inertial
39 sensors. The researchers in [9] proposed wearable sensors that help in assessing the mobility
40 impairment. In [10] the authors have focused on human upper as a link structure with 5 degree of
41 freedom. An unscented Kalman filter has been applied to the data of wearable IMU sensor to estimate
42 the upper arm and forearm movement relationship. However, the movement difference between
43 body segments and the IMU placed on corresponding skin increases significantly with intensive

44 movement. Other works have modeled geometrical constraints in elbow joint and compensate drift
 45 by fusing these constraints with particle filter [11]. Inertial sensors have been fused with several other
 46 optical motion capture systems like webcam [12] and Ms Kinect [13] and the results are validated
 47 with the golden standard system Vicon. In these work the data from optical motion capture system
 48 and inertial sensors have been fused to track trajectories and to estimate the range of motion.
 49 However, the drifting and placement issues of IMU on human body segments have been reported by
 50 many research works [7, 9, 10].

51 In recent years, researchers have used electromyography to estimate motion of upper extremity.
 52 In [14], the elbow joint angle estimation has been used to tele-operate a robot based on Surface
 53 Electromyography (sEMG) signals. The estimation of elbow joint motion has been accomplished
 54 using auto regressive moving average. The authors in [15] classified the shoulder joint motion into 4
 55 classes by quadratic discriminant analysis of EMG signals. In [16], the authors have estimated 4 DoF
 56 across upper limb, shoulder and elbow joints with simultaneous and continuous kinematics. Their
 57 results show that independent component analysis with single artificial neural network (ANN) for
 58 multiple-joint kinematics estimation is effective and feasible. Another technique for elbow angle
 59 estimation has been stated by authors in [17]. In their work, the authors estimated elbow joint with
 60 goniometer calibration and trained the developed ANN to measure the elbow joint angle from EMG
 61 signals. The EMG signals pattern are classified and recognized according to human motion to
 62 estimate elbow joint angle using neural network by many other researchers [18, 19]. The elbow joint
 63 angle estimation with sEMG signals depends on the electrodes position as well as the length of
 64 muscles (Biceps and triceps) during force [20].

65 Single RGB camera has also been used to estimate the human motion using markers. In [21], the
 66 patients gait motion has been analyzed with RGB camera with bulls-eye marker placed on neck,
 67 shoulder, waist, elbow and wrist. The markers are then tracked by the camera while the patient taking
 68 a cup of tea from desk to mouth and placing it back on the desk.

69 Most of the marker based motion estimation systems are time consuming, expensive and require
 70 calibrated and well structure environment. In this paper, we present a cost-effective markerless
 71 system to estimate elbow joint angle based on bottom-up approach in [22]. The proposed system uses
 72 a single RGB camera that requires less computational power without any calibrated environment.
 73 We have released the [code](#) for estimating the elbow angle in real time for a single person.

74 2. Neural Network Model

75 In [22], the authors proposed a bottom-up approach to estimate 2D poses of multiple human in
 76 a real-time scene. The human body segments are located and associated by means of two branches of
 77 same chronological prediction process. We have used this trained model to estimate the elbow angle
 78 for a single person using only one RGB camera.

79 A colour image of size $x \times y$ is given to the system as input, which produces the 2D locations
 80 of human body segments. Feed-forward network concurrently predicts a set of confidence maps \mathbf{P}
 81 of body segment 2D locations and a set \mathbf{Q} of part affinities field which expresses the amount of
 82 association between segments.

83 The set $\mathbf{P} = (\mathbf{P}_1, \mathbf{P}_2, \dots, \mathbf{P}_G)$ and the set $\mathbf{Q} = (\mathbf{Q}_1, \mathbf{Q}_2, \dots, \mathbf{Q}_H)$ have G confidence map and H
 84 vector field respectively one per segment where $\mathbf{P}_g \in \mathbb{R}^{x \times y}$ and $\mathbf{Q}_h \in \mathbb{R}^{x \times y \times 2}$. The neural network
 85 has been divided into two branches that makes iterative predictions over successive time values
 86 of $k \in \{1, 2, \dots, K\}$ for confidence map \mathbf{P}^k and affinity fields \mathbf{Q}^k .

87 The first ten layers of convolutional neural network in [22], first analyze the image and then produce
 88 a set of feature maps \mathbf{F} . These features maps are given as input to the first stage of each branch. A
 89 set of confidence maps $\mathbf{P}^1 = \alpha^1(\mathbf{F})$ and a set of $\mathbf{Q}^1 = \beta^1(\mathbf{F})$ affinity fields are produced by network
 90 at first stage. Where α^1 and β^1 are the CNNs for inference at Stage 1. The previous stage predictions
 91 and image features \mathbf{F} from both branches are combined in each subsequent stage and produce refine
 92 predictions.

$$93 \quad \mathbf{P}^k = \alpha^k(\mathbf{F}, \mathbf{P}^{k-1}, \mathbf{Q}^{k-1}), \forall k \geq 2 \quad (1)$$

$$94 \quad \mathbf{Q}^k = \beta^k(\mathbf{F}, \mathbf{P}^{k-1}, \mathbf{Q}^{k-1}), \forall k \geq 2 \quad (2)$$

95 Where α^k and β^k are CNNs for inference at stage k .

96 Two loss function one at each branch, are applied at the end of each stage to iteratively predict
97 confidence maps in first branch and affinity fields of human key points in second branch.
98 Specifically, at both branches the loss function at stage k is

$$99 \quad l_{\mathbf{P}}^k = \sum_{g=1}^G \sum_{\mathbf{p}} \mathbf{D}(\mathbf{p}) \cdot \|\mathbf{P}_g^k(\mathbf{p}) - \mathbf{P}_g^*(\mathbf{p})\|_2^2 \quad (3)$$

$$100 \quad l_{\mathbf{Q}}^k = \sum_{h=1}^H \sum_{\mathbf{p}} \mathbf{D}(\mathbf{p}) \cdot \|\mathbf{Q}_h^k(\mathbf{p}) - \mathbf{Q}_h^*(\mathbf{p})\|_2^2 \quad (4)$$

101 Where \mathbf{P}_g^* and \mathbf{Q}_h^* are the ground truth confidence maps and part affinity vector fields
102 respectively generated from the annotated 2D key points, \mathbf{D} is a binary mask with $\mathbf{D}(\mathbf{p}) = 0$, when
103 at location \mathbf{p} annotations are missing. The overall objective is

$$104 \quad l = \sum_{k=1}^K (l_{\mathbf{P}}^k + l_{\mathbf{Q}}^k) \quad (5)$$

105 The confidence maps for particular body parts are generated as per equation (6). Let $\mathbf{i}_g \in \mathbb{R}^2$ is
106 body segments g ground truth position. At location $\mathbf{p} \in \mathbb{R}^2$ in \mathbf{P}_g^*

$$107 \quad \mathbf{P}_g^*(\mathbf{p}) = \exp\left(-\frac{\|\mathbf{p} - \mathbf{i}_g\|_2^2}{\sigma^2}\right) \quad (6)$$

108 Let \mathbf{i}_{g_1} and \mathbf{i}_{g_2} are the body segments g_1 and g_2 groundtruth positions from the limb h . At image
109 point \mathbf{p} , the vector field \mathbf{Q}_h^* are define as

$$110 \quad \mathbf{Q}_h^*(\mathbf{p}) = \begin{cases} \mathbf{v} & \text{if } \mathbf{p} \text{ on limb } h \\ \mathbf{0} & \text{otherwise} \end{cases} \quad (7)$$

111 Where $\mathbf{v} = (\mathbf{i}_{g_2} - \mathbf{i}_{g_1}) / \|\mathbf{i}_{g_2} - \mathbf{i}_{g_1}\|_2$, is a unit vector in the limb direction. Those points which are
112 within a distance defined by the following line segment are said to be on the limb.

$$113 \quad 0 \leq (\mathbf{p} - \mathbf{i}_{g_1}) \cdot \mathbf{v} \leq r_g \text{ And } |(\mathbf{p} - \mathbf{i}_{g_1}) \cdot \mathbf{v}_{\perp}| \leq \sigma_r$$

114 Here σ_r (limb width) is the distance in pixels $r_g = \|\mathbf{i}_{g_2} - \mathbf{i}_{g_1}\|_2$ and \mathbf{v}_{\perp} is a vector perpendicular
115 to \mathbf{v} .

116 The association between the body segments is computed by the line integral over the matching
117 part affinity field, along the line segment connecting body part locations. Specifically, for two body
118 segments locations \mathbf{s}_{g_1} and \mathbf{s}_{g_2} , the predicted vector fields \mathbf{Q}_h are sampled along the line segment
119 to estimate the confidence in their association.

$$120 \quad Z = \int_{a=0}^{a=1} \mathbf{Q}_h(\mathbf{p}(a)) \cdot \frac{\mathbf{s}_{g_2} - \mathbf{s}_{g_1}}{\|\mathbf{s}_{g_2} - \mathbf{s}_{g_1}\|_2} da \quad (8)$$

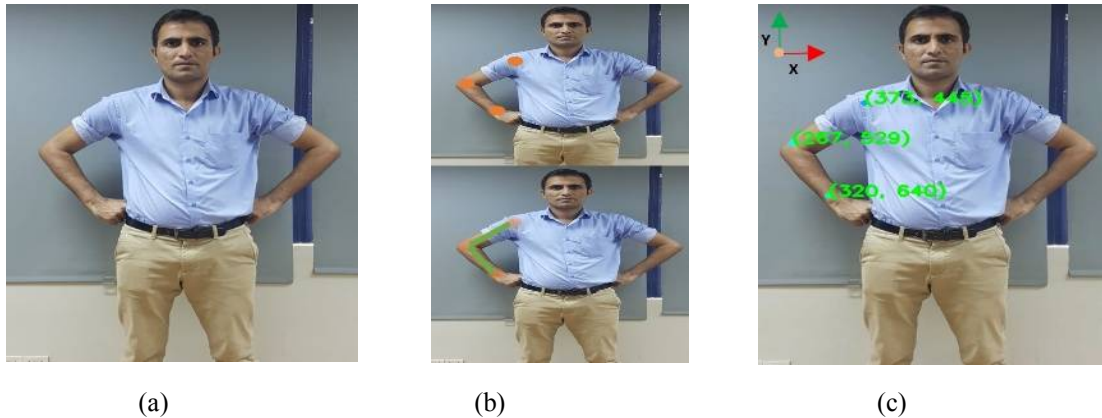
121 Where $\mathbf{p}(a)$ interpolates the position of the two body segments \mathbf{s}_{g_1} and \mathbf{s}_{g_2} .

122 Equation 8 defines the score of each body limb using the line integral calculation. Thus, we
123 obtain a set of body part detection for a single person.

124 3. Elbow Angle Calculation

125 The image captured through RGB camera is passed through trained model, the confidence map
126 for upper limb joints locations are estimated and are associated through part affinity filed. After
127 confidence map estimation and vector field association, the three joints coordinates are extracted
128 for angle estimation as shown in Figure-1 (c).

129 The Elbow angle is estimated with RGB camera and its results are then compared with
130 Microsoft Kinect in Results section.



131 (a) (b) (c)
132 **Figure-1** Shows overall process. (a) Input image, (b) Two-branch CNN to predict confidence maps for upper limb
133 segments and vector fields for segments association. (c) Joints location coordinates are extracted and are used to
134 estimate elbow angle

135 4. Methodology

136 Figure-2 shows the overall process from acquisition to angle estimation for both motion capture
137 system. The camera sends thirty frames per second to the trained neural network model. Two
138 branches of neural networks predict the confidence map and vector field simultaneously in a single
139 layer. Once the body parts 2D position and orientation are localized, then the coordinates of the
140 human anatomical parts are extracted from the frames using body's center of mass as region. The
141 coordinates of shoulder, elbow and wrist of right limb respectively are processed for angle
142 calculation. The elbow angle is estimated from the vector transformation of these coordinates using
143 the following formula.

$$144 \quad \mathbf{u} = \mathbf{x}_s - \mathbf{x}_e$$

$$145 \quad \mathbf{v} = \mathbf{x}_w - \mathbf{x}_e$$

$$146 \quad \theta = \cos^{-1} \left(\frac{\langle \mathbf{u}, \mathbf{v} \rangle}{\|\mathbf{u}\| \|\mathbf{v}\|} \right)$$

147 Where \mathbf{x}_s , \mathbf{x}_e and \mathbf{x}_w are the coordinate vectors for shoulder, elbow and wrist joints respectively.

148 While $\langle \cdot, \cdot \rangle$ denotes the inner product and $\|\cdot\|$ is the l_2 norm of the vector.

149 Microsoft Kinect acquires 3D depth images by using built-in infrared projector and
150 complementary metal oxide semiconductor sensor to track human body-joint motion in real time
151 [23]. We use the same mathematical formula for estimating elbow joint angle with Kinect as for RGB
152 camera.

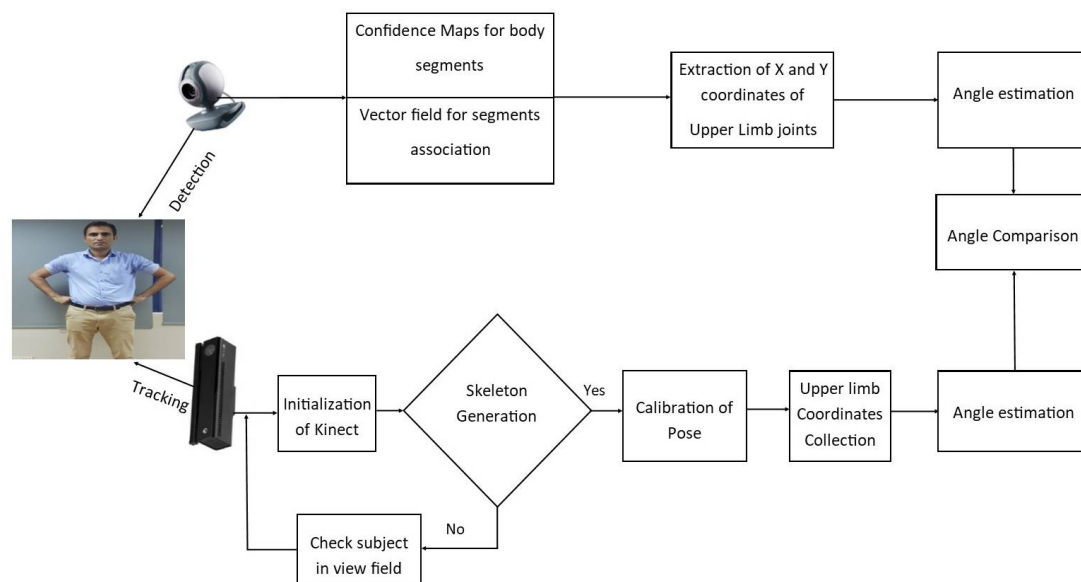
153 Ms Kinect tracks the human skeleton with a 30 frames per second while the RGB camera is
154 using 15 frames per second. We synchronized the frames from both system with respect to time in
155 milliseconds. So it synchronizes all those frames of RGB camera which are having matching time with
156 that of Ms Kinect frames. The pseudo code for synchronizing RGB camera with Microsoft Kinect
157 based on time matching frames is as follow,

- 158 1. **START**
- 159 2. **INPUT:** KDataCollection, Kinect angle data w.r.t time
- 160 3. RGBDataClllection, RGB camera angle data w.r.t time
- 161 4. **OUTPUT:** synDataCollection, Merged Data for Kinect and RGB angles w.r.t to time
- 162 5. **INITIALIZE:** KinectTime, store current Kinect time

```

163         6.           RGBTime, store current RGBCamera time
164         7.   FOREACH Kdata in KDataCollection
165         8.     SET KinectTime = Kdata [Time]
166         9.     FOREACH RGBData in RGBDataCllection
167         10.    SET RGBTime = RGBData [Time]
168         11.    IF KinectTime = RGBTime THEN
169         12.      synDataCollection.Add (KinectTime, Kdata[Angle],RGBData [Angle])
170         13.    END IF
171         14.  END FOREACH
172         15. END FOREACH
173         16. RETURN synDataCollection
174         17. STOP

```



175 **Figure-2** overall process for Estimation of Elbow angle

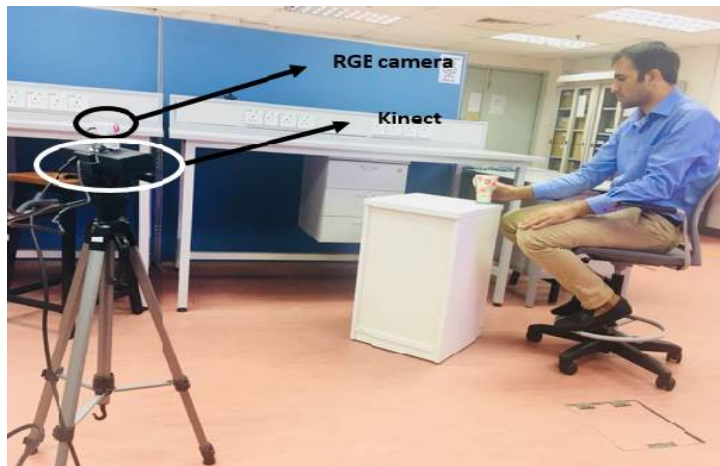
176 4.1 participants

177 For angle estimation, we performed cup to mouth action on five participants (height, 168 ± 8 cm;
 178 mass, 61 ± 17 kg). The participants take part voluntarily after taking ethical approval from Unkl
 179 Research Ethics Committee. Written consent was obtained before data acquisition and all participants
 180 were having no injury.

181 4.2. Experimental setup

182 In our experiment, we engaged five healthy subject and didn't use any markers for tracking the
 183 movement of subject's body. A single experiment consists of three trails for each subject. During
 184 each trail, the subject was seated on a chair and asked to perform the experiment by lifting a cup
 185 from table and moving it near to the mouth. The cup was then brought back it to its initial position.
 186 During the entire trial, both RGB camera as well as Ms Kinect track the joints coordinates in real
 187 time to compute the estimated angles independently in Sagittal and coronal planes.

188 The experimental design reflects the movement related to the daily activities. In rehabilitation
 189 systems, this task plays an important role to track the motion in degrees where therapist can gauge
 190 patient performance based on the data acquired.



191 **Figure-3.** Experimental setup

191

192 5. Software setup

193 Microsoft kinect was programmed using C# with Coding4fun toolkit [24] to estimate the elbow
 194 joint angle. The angle estimation for the frames captured through RGB camera was done using
 195 python. Both of these motion capture systems were used to track human body simultaneously in real
 196 time. However, Ms Kinect acquires three coordinates while RGB camera acquires two coordinates for
 197 shoulder, elbow and wrist joint. Similarly, the Microsoft kinect has a frame rate of 30 frame per second
 198 whereas RGB camera has a frame rate of 15 frame per second. To adjust the frame rates, the frames
 199 of RGB camera are synchronized with Microsoft kinect with respect to time (within millisecond
 200 accuracy) by down sampling Microsoft kinect frame rate. To get an accurate comparison of the two
 201 motion capture systems, the analysis has been done using the results after synchronization.

202 5. Result and Discussion

203 Initially the subject was asked to make a static pose in two different planes i.e. sagittal and
 204 coronal to compare the accuracy of elbow joint angle measured through RGB camera and MS Kinect.
 205 It can be seen from figure-4 that the angles estimated through both systems are nearly equal. The
 206 results depicted in fig-4 (a) shows the accuracy of the angles computed through RGB camera and Ms
 207 Kinect in the sagittal plane which are 152.27° and 150° respectively. In a separate experiment,
 208 carried out in the coronal plane, the angle recorded by RGB camera is 38.55° which is again
 209 approximately equal to that measured by MS Kinect i.e. 39° .

210

211

212

213

214

215

216

217

218

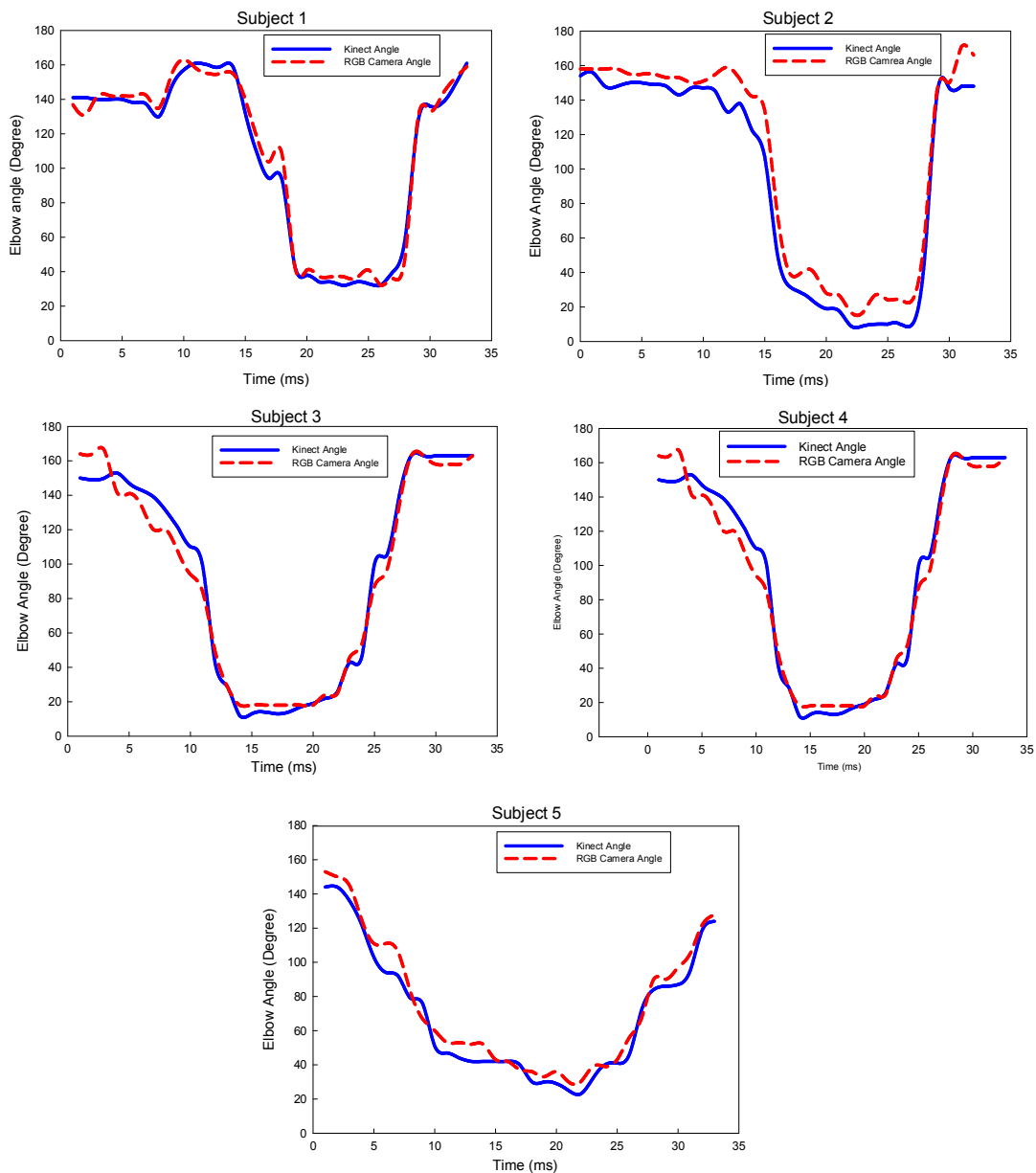


219

220

Figure-4. Shows angle estimation in two different static poses by RGB camera and Ms Kinect. The angle in black color on left side of both (a) and (b) is of Ms Kinect and angle in blue color is of RGB camera.

221
222
223
224

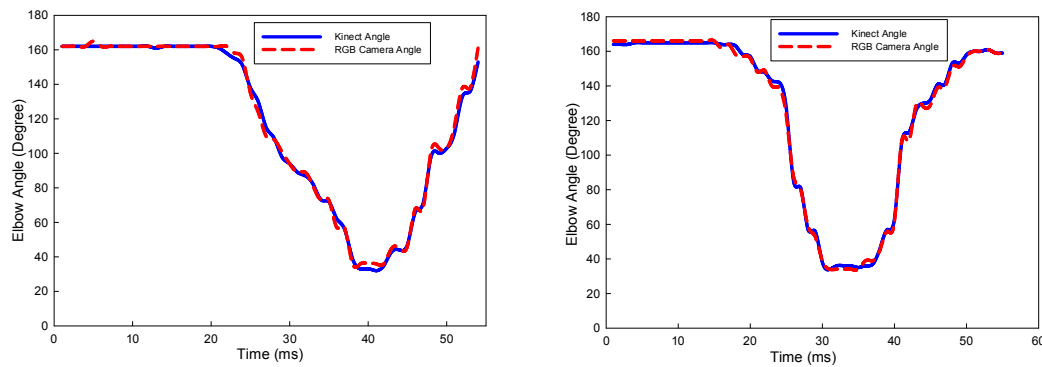


225
226
227
228
229
230
231
232
233
234
235
236
237
238
239

Figure-5. Elbow angle measured in degree by RGB camera and Microsoft Kinect in sagittal plane.

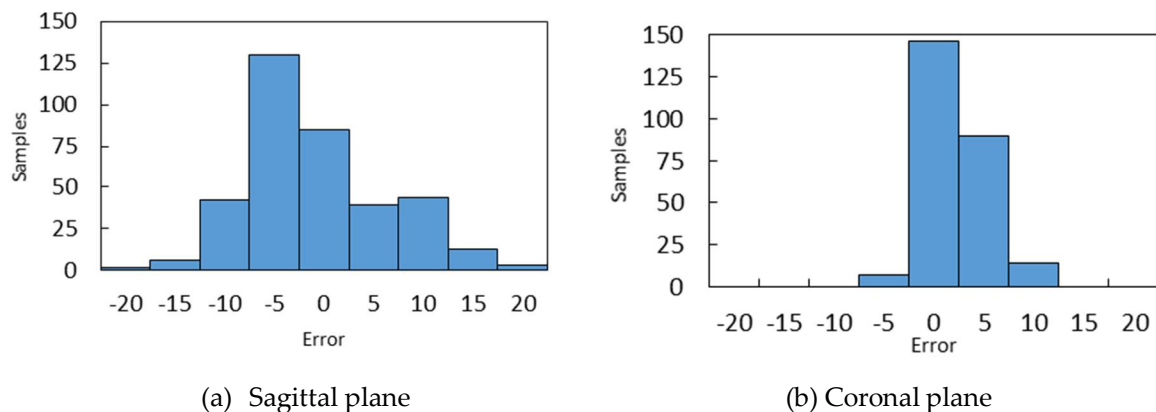
240 After the static pose trail, the subject was asked to perform cup to mouth experiment in both
241 Sagittal and coronal planes to record the motion trajectory. Figure-5 shows the results of elbow joint
242 angle estimated for each of the subject in the Sagittal plane. The motion trajectory shown is based on
243 a single trial for the timely synchronized frames of both motion capturing systems. It can be seen
244 from the results that the elbow joint angles calculated during motion with RGB camera nearly follow
245 the results of MS Kinect for all the subjects.

246 The motion trajectories of elbow joint angle performing the same task in coronal plane are shown
247 in Figure-6. It is evident that the results in coronal plane are quite promising as compared to those in
248 sagittal plane (Figure-5) due to precise position detection of the wrist joints coordinates.



249
250 **Figure-6.** Estimates elbow angle in degrees with RGB camera and Microsoft Kinect in coronal plane for
251 two trails.

252 Figure-7 illustrates error histograms from the angle estimated by RGB camera and Microsoft
253 Kinect in sagittal and coronal plane. The errors are computed after synchronizing the frames of RGB
254 camera and Ms Kinect. The error range in sagittal plane is between $\pm 10^\circ$ due to imprecise detection
255 of the wrist joint. While, in coronal plane wrist joint is precisely detected and showing the lesser range
256 of error. The median of Root Mean Square Error (RMSE) for sagittal and coronal planes is given in
257 table-1 for all the subjects.



258 (a) Sagittal plane (b) Coronal plane
259 **Figure-7.** Error histogram of RGB camera and Microsoft Kinect

260 Experimental results show that the use of a single RGB camera can be a cost-effective alternative
261 solution to Ms Kinect for estimating joint elbow angles in applications like rehabilitation etc.
262
263
264
265

Table-1. RMSE in frames of RGB camera w.r.t Microsoft Kinect in sagittal and coronal plane

Subject	Sagittal plane(RMSE)	Coronal Plane(RMSE)
1	1.5°	1°
2	4°	2°
3	2°	0.5°
4	2.5°	0.5°
5	3.5°	1°

266 267 6. Conclusions

268 The comparison of RGB camera with Ms Kinect is a key aspect for the development of low cost
269 markerless motion capture system. This paper illustrates the exploration and evaluation of tracking

270 motion accuracy amongst low cost RGB camera and Ms Kinect. Markerless RGB camera based
 271 motion capture system has shown reasonably accurate results in coronal plane and can be used to
 272 estimate joint elbow angle in rehabilitation.

273 Future studies should address the wrist joint position detection issues in sagittal plane. The
 274 proposed work can be used in other areas for movement-based experiments such as motion analysis
 275 of athletes, posture estimation, security camera and many more.
 276

277 **Acknowledgments :** This research has been generously supported by a research grant by the Ministry of
 278 Science, Technology and Innovation (MOSTI) under the Program Flagship DSTIN for the development of a
 279 new technology identified as "Building Our Robotic Competitiveness in Medical Healthcare: Development of
 280 Robots for Assisted Recovery and Rehabilitation".

281 **Author Contributions:** Muhammad Yahya raised up the idea and wrote the paper. Jawad Ali Shah
 282 supervised the whole process. Arif Warsi helped to develop the code. The results were discussed, validated
 283 and modified by Kushsairy Kadir. Sheroz khan and Izani done analysis.

284 **Conflicts of Interest:** I declare that there is no conflict with other research work.

285 References

- 286 1. Mohamed, Hussein, Ali Ahmed, Mostafa. R. "Motion Control of Robot by using Kinect Sensor."
 287 (2014): 1-5.
- 288 2. Kanesalingam. T, "Motion Tracking Glove for Human-Machine Interaction: Inertial Guidance,"
 289 2010.
- 290 3. Knippenberg E, Verbrugghe J, Lamers. I, Palmaers. S, Timmermans. A, Spooren. A, "Markerless
 291 motion capture systems as training device in neurological rehabilitation: a systematic review of
 292 their use, application, target population and efficacy," *Journal of neuroengineering and
 293 rehabilitation*, vol. 14, p. 61, 2017.
- 294 4. Bonnechère, B., Sholukha, V., Omelina, L., Van, S. S. J., & Jansen, B. (2018). 3D Analysis of Upper
 295 Limbs Motion during Rehabilitation Exercises Using the Kinect™ Sensor: Development,
 296 Laboratory Validation and Clinical Application. *Sensors (Basel, Switzerland)*, 18(7).
- 297 5. A. Cappozzo, F. Catani, A. Leardini, M. Benedetti, and U. Della Croce, "Position and orientation
 298 in space of bones during movement: experimental artefacts," *Clinical biomechanics*, vol. 11, pp.
 299 90-100, 1996.
- 300 6. J. Fuller, L.-J. Liu, M. Murphy, and R. Mann, "A comparison of lower-extremity skeletal
 301 kinematics measured using skin-and pin-mounted markers," *Human movement science*, vol. 16,
 302 pp. 219-242, 1997.
- 303 7. P. Müller, M.-A. Bégin, T. Schauer, and T. Seel, "Alignment-free, self-calibrating elbow angles
 304 measurement using inertial sensors," in *Biomedical and Health Informatics (BHI), 2016 IEEE-EMBS
 305 International Conference on*, 2016, pp. 583-586.
- 306 8. Mousavi Hondori. H, Khademi.M, "A review on technical and clinical impact of microsoft kinect
 307 on physical therapy and rehabilitation," *Journal of medical engineering*, vol. 2014, 2014.
- 308 9. Y. Moon, R. S. McGinnis, K. Seagers, R. W. Motl, N. Sheth, J. A. Wright Jr, *et al.*, "Monitoring gait
 309 in multiple sclerosis with novel wearable motion sensors," *PLoS One*, vol. 12, p. e0171346, 2017.
- 310 10. Zhang ZQ, Wong WC, Wu JK. Ubiquitous human upper-limb motion estimation using wearable
 311 sensors. *IEEE Transactions on Information technology in biomedicine*. 2011 Jul; 15(4):513-21.
- 312 11. Zhang Z, Huang Z, Wu J. Hierarchical information fusion for human upper limb motion capture.
 313 *In Information Fusion, 2009. FUSION'09. 12th International Conference on* 2009 Jul 6 (pp. 1704-
 314 1711). IEEE.
- 315 12. Y. Tao and H. Hu, "A novel sensing and data fusion system for 3-D arm motion tracking in
 316 telerehabilitation," *IEEE Transactions on Instrumentation and Measurement*, vol. 57, pp. 1029-1040,
 317 2008.

- 318 13. Y. Tian, X. Meng, D. Tao, D. Liu, and C. Feng, "Upper limb motion tracking with the integration
319 of IMU and Kinect," *Neurocomputing*, vol. 159, pp. 207-218, 2015.
- 320 14. P. K. Artemiadis and K. J. Kyriakopoulos, "EMG-based teleoperation of a robot arm in planar
321 catching movements using ARMAX model and trajectory monitoring techniques," in *Robotics
322 and Automation, 2006. ICRA 2006. Proceedings 2006 IEEE International Conference on*, 2006, pp. 3244-
323 3249.
- 324 15. Ehrampoosh A, Yousefi-Koma A, Mohtasebi SS, Ayati M. EMG-based estimation of shoulder
325 kinematic using neural network and quadratic discriminant analysis. In *Robotics and
326 Mechatronics (ICROM), 2016 4th International Conference on* 2016 Oct 26 (pp. 471-476). IEEE.
- 327 16. Q. Zhang, R. Liu, W. Chen, and C. Xiong, "Simultaneous and continuous estimation of shoulder
328 and elbow kinematics from surface EMG signals," *Frontiers in neuroscience*, vol. 11, p. 280, 2017.
- 329 17. S. Suryanarayanan, N. Reddy, and V. Gupta, "Artificial neural networks for estimation of joint
330 angle from EMG signals," in *Engineering in Medicine and Biology Society, 1995., IEEE 17th Annual
331 Conference*, 1995, pp. 823-824.
- 332 18. Desplenter T, Trejos AL. Evaluating Muscle Activation Models for Elbow Motion Estimation.
333 *Sensors*. 2018 Mar 28;18(4):1004.
- 334 19. Tang Z, Zhang K, Sun S, Gao Z, Zhang L, Yang Z. An upper-limb power-assist exoskeleton using
335 proportional myoelectric control. *Sensors*. 2014 Apr 10;14(4):6677-94.
- 336 20. E. P. Doheny, M. M. Lowery, D. P. FitzPatrick, and M. J. O'Malley, "Effect of elbow joint angle
337 on force-EMG relationships in human elbow flexor and extensor muscles," *Journal of
338 Electromyography and Kinesiology*, vol. 18, pp. 760-770, 2008.
- 339 21. C. Yang, A. Kerr, V. Stankovic, L. Stankovic, and P. Rowe, "Upper limb movement analysis via
340 marker tracking with a single-camera system," in *Image Processing (ICIP), 2014 IEEE International
341 Conference on*, 2014, pp. 2285-2289.
- 342 22. Z. Cao, T. Simon, S.-E. Wei, and Y. Sheikh, "Realtime multi-person 2d pose estimation using part
343 affinity fields," *arXiv preprint arXiv:1611.08050*, 2016.
- 344 23. Fern'ndez-Baena, A., Sus'ın, A. and Lligadas, X., 2012, September. Biomechanical validation of
345 upper-body and lower-body joint movements of kinect motion capture data for rehabilitation
346 treatments. In *Intelligent networking and collaborative systems (INCoS), 2012 4th international
347 conference on* (pp. 656-661). IEEE.
- 348 24. Coding4Fun Kinect Toolkit - Toolkit Download' <https://c4fkinect.codeplex.com/>